TuijinJishu/Journal of Propulsion Technology
ISSN: 1001 -4055
Vol. 44 No. 5 (2023)

Influence of Variable Viscosity and Prandtl Number on MHD Unsteady Natural Convection on a Thin Vertical Cylinder

[1]Roopadevi K. N [2]A.H. Srinivasa [3]A.T. Eswara

[1][3]Research Centre, Department of Mathematics, GSSS Institute of Engineering and Technology for Women, Mysuru-570 016, India
[2]Research Centre, Department of Mathematics, Maharaja Institute of Technology, Mysore 570018, India

Abstract: This present work explores the effect of variable viscosity and Prandtl number on unsteady free convection of methanol flow over a thin vertical cylinder with magnetic field. The governing flow equations of the flow are transformed into dimensionless partial differential equations using non-similar transformations. The converted equations are resolved by employing implicit finite difference scheme and quasilinearization technique. To see a better perception of the problem, the numerical solutions so obtained are analysed graphically, thereby examining the impact of variable viscosity and Prandtl number on friction drag and heat transfer parameters. We also examined the impact of physical parameters like unsteady, magnetic, and stream-wise coordinate on friction drag, heat transfer, temperature and velocity profile.
Keywords: Unsteady, Variable viscosity, Prandtl number, MHD, Cylinder.

1. Introduction

Heat transfer by free convection often occurs in various industrial applications and physical problems, such as fiber and granular insulation, geothermal systems, the stars and planets structure analysis, the nuclear reactors cooling etc. The flow analysis of electrically conducting fluid with magnetic field has drawn attention from several scholars' owing to its versatile applications. Both in geophysics and astrophysics, it is to analyse the stellar and solar structures, interstellar matter and radio propagation through the ionosphere. The importance of fluid flow over a thin vertical cylinder with unsteady axial velocity, thermal conductivity and temperature dependent viscosity under a uniform normal magnetic field can be seen in many engineering applications like the glass and polymer industries, exploration and thermal recovery of oil, geothermal reservoirs, underground nuclear waste storage sites and in the assessment of aquifers etc.,

Surma Devi[1] premeditated heat conduction effect in steady free convection over a vertical cylinder, applying an implicit finite difference scheme. Free convection flow on a vertical cylinder embedded in a thermally stratified high porosity medium problem was considered by Takhar[2]. An analysis of unsteady natural convection flow with temperature dependent thermal conductivity past an isothermal vertical cylinder using explicit finite difference method is discussed by Md. A Hossain[3]. Rani[4] considered the outcome of the couple stress parameter and Prandtl number on the transient free convection flow over a vertical cylinder. Loganathan[5] an unsteady free convection flow over a moving vertical cylinder with temperature oscillations in the presence of porous medium. The flow behaviour and heat and mass transfer chactericstic of unsteady free convection flow past a vertical cylinder with magnetic field is discussed by Periyana Gounder Ganesan [6]. The behaviour of unsteady couple stress fluid flow about a cylinder with magnetic force under thermal radiation and viscous dissipation effects is investigated by Suresha Suraiah Palaiah [7]

All aforementioned research works are restricted to constant fluid properties. As we know, certain physical properties of the fluid change with temperature, particularly viscosity and thermal conductivity. Since then, several works pertaining to variable viscosity with different parameters and distinct geometry have been endeavoured by several researchers [8-14] by taking that viscosity varies as an inverse function of temperature. Pantokratoras [15] considered the steady laminar flow over continuous moving flat plate by considering variable viscosity and varying Prandtl number across the boundary layer. The steady laminar non-similar boundary layer forced convection flow over a yawed infinite circular cylinder is investigated by Saikrishnan Ponnaiah[16]. Abhishek Kumar Singh et al. [17] continued the work by considering the flow over a moving vertical plate. Recently Rooadevi et al..[19] considered the problem variable viscosity and Prandtl number effect on MHD unsteady free convection axisymmetric ethanol boundary-layer flow. As viscosity varies with temperature and Prandtl number depend on viscosity, in the preceding research works [17,18,19] researcher considered viscosity and Prandtl number as functions of temperature.

From all these works, it is clear that, variable viscosity and Prandtl number have been taken into consideration with various geometries along with steady or unsteady natural or mixed convection flow. Apropos of all these works, we considered the variable viscosity and Prandtl number influence on unsteady free convection flow over a thin cylinder with magnetic field. Particularly methanol fluid is considered as a working fluid as it is multipurpose fuel, it can be used directly or as a blending component in fuels, produced from ash coal, agricultural residue and natural gases.

Table 1. Thermo-physical properties value of methanol at different temperatures [19,20]

Temperature (T^0C)	**Density** (ρ) **(gr./ cm^3)**	**Thermal conductivity** (k) $(erg \times 10^5/cm.s^0K)$	**Specific heat**(c_p) $(J \times 10^7/kg^0K)$	**Viscosity**(μ) $(\mathrm{gr.} \times 10^{-2}\mathrm{cm.\,s})$	**Prandtl number** (Pr)
00.0	0.813	0.207	2.399	0.777	9.005
10.0	0.804	0.204	2.449	0.664	7.971
20.0	0.794	0.201	2.504	0.575	7.163
30.0	0.785	0.199	2.566	0.504	6.498
40.0	0.775	0.196	2.633	0.447	6.004
50.0	0.765	0.193	2.706	0.399	5.594

2. Mathematical analysis

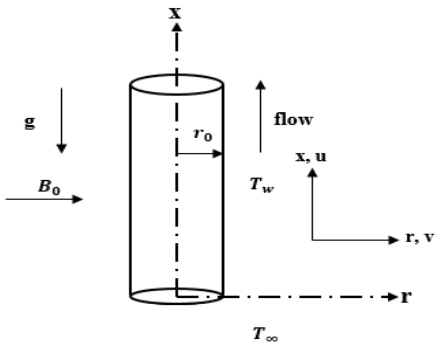

Figure 1. Diagram and coordinate system of the flow

Let us consider an unsteady laminar viscus incompressible free convection flow of an electrically conducting methanol fluid past a thin vertical cylinder with transvers magnetic field B_0. Figure 1 shows the geometrical representation of the flow analysis. The cylinder of radius r_0 is situated in a quiescent atmosphere having temperature T_∞ and the surface temperature of the cylinder T_w. The axial coordinate is taken as x, measuring the distance from the centre line of the cylinder to its bottom end. That is from the statting edge of cylinder where the thickness of boundary layer is zero. The radial co-ordinate r is taken perpendicular to the x axis and gravitational force 'g' is measured opposite to the x axis. Initially (i.e., time $t = 0$) both cylinder and surrounding fluid are maintained at constant temperature. When time $t > 0$ the temperature of the cylinder is changed to $T_w = T_w + \varepsilon\Delta T_w$. (i. e. , $T_w > T_\infty$) and the same is maintained with $\varepsilon > 0$, creating unsteadiness. As the heat created by compression of the fluid is very small, it is ignored. To minimize ($\leq 40^0C$) surface and free stream temperature difference, the ambient fluid temperature is taken , $T_\infty = 28.0^0C$ and $\Delta T_w = 10^0C$. Under the aforementioned assumptions and Boussinesq boundary layer approximation for the incompressible fluid model, the governing equations of the viscous fluid [1] are

$$\frac{\partial(ru)}{\partial x} + \frac{\partial(rv)}{\partial y} = 0 \tag{1}$$

$$\frac{\partial u}{\partial t} + u\frac{\partial u}{\partial x} + v\frac{\partial u}{\partial r} = g\beta(T - T_\infty) + \frac{1}{r\rho_\infty}\frac{\partial}{\partial r}\left(\mu r\frac{\partial u}{\partial r}\right) - \frac{\sigma {B_0}^2 u}{\rho} \tag{2}$$

$$\frac{\partial T}{\partial t} + u\frac{\partial T}{\partial x} + v\frac{\partial T}{\partial r} = \frac{1}{r\rho_\infty}\frac{\partial}{\partial r}\left[\left(\frac{\mu r}{Pr}\frac{\partial T}{\partial r}\right)\right] \tag{3}$$

with the boundary conditions:

$$\begin{aligned} &u = 0, v = 0, T = 0 \text{ or } T = T_\infty \quad \text{for} \quad t \leq 0, \forall\, x \; and \; r \\ &u = 0, v = 0, T = 1 \text{ or } T = T_w \quad \text{for } t > 0 \; at \; r = r_0 \\ &u = 0, v = 0, T = 0 \text{ or } T = T_\infty \quad \text{at } x = 0 \\ &u \to 0, v \to 0, T = 0, \quad t \to T_\infty \; and \; r \to \infty \end{aligned} \tag{4}$$

Here u and v respectively represents the velocity components along x and r directions, ν is the dynamic viscosity, β is the thermal expansion coefficient, T is the fluid temperature, Pr Prandtl number, ρ is the density, σ electrical conductivity. Here we considered except viscosity all other thermo physical properties of fluid as constant, however Prandtl number varies with the viscosity, both Prandtl number (Pr) and viscosity (μ) are considered as inverse linear function of temperature[19].

$$\mu = 1/(b_1 + b_2T)\,;\; Pr = 1/(c_1 + c_2T) \tag{5}$$

$$\text{where, } b_1 = 126.23, \quad b_2 = 2.438, \quad c_1 = 0.1109 \quad \text{and} \quad c_2 = 0.0013 \tag{6}$$

We have taken the statistics from Ref [19,20,21]to correlate the above values. Equations (1) and (2) hold good approximately for the liquids having small temperature difference between ambient and wall.

The subsequent dimensionless transformations are introduced to analyse the equations (1) -(3)

$$\psi(\eta, \xi, t^*) = 4\nu r_0\left({}^{x}/_{r_0}\right)^{3/4}(Gr)^{1/4}[f(\xi, \eta, t^*)];\; t^* = \frac{t\nu}{{r_0}^2};$$

$$\mathrm{M} = \frac{\sigma {B_0}^2 {r_0}^{3/2} x^{1/2}}{\rho (Gr)^{1/2}};\ u = \frac{1}{r}\frac{\partial \psi}{\partial \mathrm{x}};\ \mathrm{v} = \frac{1}{r}\frac{\partial \psi}{\partial \mathrm{r}}$$

$$T = T_\infty + (T_w - T_\infty)G(\eta, \xi, t^*);\quad \eta = \frac{(Gr)^{1/4}(r^2 {r_0}^{-2} - 1)}{2\left(x/r_0\right)^{1/4}};\quad \xi = 2\left(x/r_0\right)^{1/4}(Gr)^{-1/4};$$

$$Gr = \frac{g\beta {r_0}^3 (T_w - T_\infty)}{4\nu^2};\quad Gr_x = \frac{g\beta x^3 (T_w - T_\infty)}{\nu^2} \tag{7}$$

Here Gr_x , Gr are respectively local Grashof number and Grashof number, M is the magnetic field

Now the Equations (2) and (3) respectively reduced to the dimensionless form as

$$(N(1+\eta\xi)F')' + 3fF' + G - 2F^2 - MF - \frac{\xi^2}{4}F_{t^*} = \xi\left(FF_\xi - F' f_\xi\right) \tag{8}$$

$$\left(N\,Pr^{-1}(1+\eta\xi)\,G'\right)' + 3fG' - \frac{\xi^2}{4}G_{t^*} = \xi\left(FG_\xi - G'^{f_\xi}\right) \tag{9}$$

and the corresponding non-dimensional initial and boundary conditions are

$$f = 0;\ F = 0;\ G = 0\ \forall\ \xi, \eta, for\ t^* \le 0$$
$$F = 0;\ G = 1 + \varepsilon\ \ at\ \eta = 0\,, \xi \ge 0, t^* \ge 0$$
$$F = 0;\ G = 0\ \ as\ \eta \to \infty\ \xi \ge 0, t^* \ge 0 \tag{10}$$

where,

$$u = \frac{4\nu(Gr)^{1/2}\left(x/r_0\right)^{1/2}}{r_0}F;$$

$$v = \frac{4\nu(Gr)^{1/4}}{r_0}\left(\frac{3}{4}\left(x/r_0\right)^{-1/4}f - \frac{1}{8}(Gr)^{1/2}\left(x/r_0\right)^{-1/2}\ (r^2 {r_0}^{-2} - 1)F + \frac{1}{2}(Gr)^{1/4}f\right);$$

$$f = \int_0^\eta F d\eta\,; N = \left(\frac{\mu}{\mu_\infty}\right) = \frac{1}{1 + a_1 G};\ Pr = \frac{1}{a_2 + a_3 G}$$

where

$$a_1 = \left(\frac{b_2}{b_1 + b_2 T_\infty}\right)\Delta T_w;\quad a_2 = c_1 + c_2 T_\infty;\quad a_3 = c_2 \Delta T_w;\quad \Delta T_w = (T_w - T_\infty);$$
$$F = \frac{\partial f}{\partial \eta};\quad \frac{\partial F}{\partial \eta};\quad G' = \frac{\partial G}{\partial \eta} \tag{11}$$

From the several engineering application point of view, the vital physical quantities the friction drag (skin friction) coefficient and Nusselt number respectively expressed as

$$C_f (Gr_x)^{1/4} = \frac{2\tau_w}{\rho_\infty r_0 U} = \frac{2\mu_\infty}{r_0 U \rho_\infty}\left(\frac{\partial u}{\partial r}\right)_{r=r_0} = \xi(F')_{\eta=0} \tag{12}$$

$$Nu(Gr_x)^{-1/4} = \frac{-x}{(T_{w0} - T_\infty)}\left(\frac{\partial T}{\partial y}\right)_{y=0} = \quad -\frac{1}{\sqrt{2}}(G')_{\eta=0} \tag{13}$$

where, $U = g\beta(T_w - T_\infty)^{5/4}\ \frac{x^{3/4}}{\nu^{1/2}}$ is a hypothetical or equivalent velocity function

3. Numerical Analysis

The coupled non-linear governing equations (8) and (9) with the boundary conditions (10) have been solved numerically using implicit finite difference scheme in conjunction with quasilinearization technique. After applying quasilinearization method, we get the linear partial differential equations as

$$F''^{(s+1)} + X_1{}^{(s)}F'^{(s+1)} + X_2{}^{(s)}F^{(s+1)} + X_3{}^{(s)}F_\xi{}^{((s+1)} + X_4{}^{(s)}F_{t^*}{}^{(s+1)} + X_5{}^{(s)}G'^{(s+1))} + X_6{}^{(s)}G^{(s+1)} = U_1{}^{(s)} \quad (14)$$

$$G''^{(s+1)} + Y_1{}^{(s)}G'^{(s+1)} + Y_2{}^{(s)}G^{(s+1)} + Y_3{}^{(s)}G_\xi{}^{(s+1)} + Y_4{}^{(s)}G_{t^*}{}^{(s+1))} + Y_5{}^{(s)}F^{(s+1)} = U_2{}^{(s)} \quad (15)$$

As it is finite implicit difference scheme, the co-efficient function with index $(s+1))$ to be found using known co-efficient function with index (s).The corresponding boundary conditions are given by

$$f^{(s+1)} = 0;\ F^{(s+1)} = G^{(s+1)} = 0\ \forall\, \xi, \eta, t^* \le 0$$
$$F^{(s+1)} = 0;\ G^{(s+1)} = 1 + \varepsilon\ \ at\ \ \eta = 0, \xi \ge 0, t^* \ge 0$$
$$F^{(s+1)} = 0;\ G^{((s+1))} = 0\quad as\ \ \eta \to \infty, \xi \ge 0, t^* \ge 0 \quad (16)$$

The co-efficient of (13) and (14) equations are

$$X_1{}^{(s)} = -\frac{a_1 G'}{ME} + NE\left(\xi + ME(\xi f_\xi + 3f)\right);\ X_2{}^{(s)} = (ME)(NE)(-4F - M - \xi F_\xi)$$
$$X_3{}^{(s)} = -\xi F(ME)(NE);\quad X_4{}^{(s)} = -(ME)(\mathrm{NE})$$
$$X_5{}^{(s)} = -\frac{a_1 F'}{(ME)}\quad ;\quad X_6{}^{(s)} = \frac{{a_1}^2 F' G'}{(ME)^2} + NE(a_1(3fF' + \xi f_\xi F' + G - 2F^2 - MF - \xi F_\xi F - \frac{\xi^2}{4}F_{t^*}) + (ME))$$
$$U_1{}^{(s)} = -\frac{a_1 F' G'}{(ME)} - (2F^2 + \xi F_\xi F + G)(ME)(NE) + X_6{}^{(q)}G$$
$$Y_1{}^{(s)} = \frac{-2a_1 G'}{(ME)} + Pr\left(2a_3 G' + (ME)(NE)\left(3f + \xi f_\xi\right)\right) + \xi(NE)$$
$$Y_2{}^{(s))} = \frac{{a_1}^2 G'^2}{(ME)^2} - {a_3}^2 G'^2 Pr^2 + (NE)(G'(3f + \xi f_\xi) - \xi F G_\xi - \frac{\xi^2}{4}G_{t^*})(a_1 Pr - a_3(ME)Pr^2)$$
$$Y_3{}^{(s)} = -(NE)(ME)\xi F Pr\ ;\ Y_4{}^{(s)} = -(NE)(ME)Pr$$
$$Y_5{}^{(s)} = -(NE)(ME)\xi G_\xi Pr;$$
$$U_2{}^{(s)} = -\frac{a_1 G'^2}{(ME)} + a_3 G'^2 Pr - (NE)(ME)Pr\xi G_\xi F + Y_2{}^{(q)}G$$

where, $ME = (1 + a_1 G)$, $NE = \frac{1}{(1+\eta\xi)}$

In each iteration, the partial differential equations (14) and (15) were stated in finite difference form, in every stage, the expressions so obtained were then changed into a system of linear algebraic equations. These equations then taken in a block tridiagonal matrix which can be resolved using Varga's technique [21].

4. Results and discussions

Employing the preceding section numerical method for the governing equations, the computation has been carried out for various parameters like axial distance, magnetic field and unsteady. To see the physical insights of the temperature profile, velocity profile, friction drag and heat transfer along with variable viscosity and Prandtl number, the graphs are plotted using the computed values of the respective. To conform the method's accuracy the results obtained for the ratio of local Nusselt

numbers, $(Nu_x/(Nu_x)_{\xi=0})$ is compared with result of Surma Devi[1] and the same is displayed in Table 2. The results are in better agreement with them.

Table 2. Comparison of $Nu_x/(Nu_x)_{\xi=0}$ result for $t^* = 0, N = 1$ and $Pr = 0.7$ with the result reported by Surma Devi[1]

ξ	$Nu_x/(Nu_x)_{\xi=0}$	
	Surma Devi [4]	Present
0	1.000	1.000
0.503	1.2101	1.2076
1.064	1.4219	1.4607
2.093	1.7782	1.8142
3.364	2.1769	2.1606

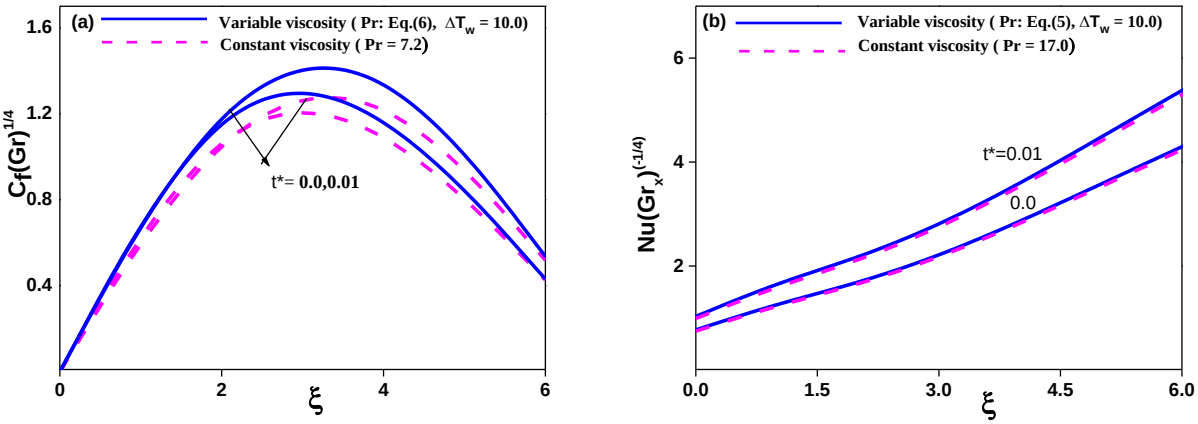

Figure 2. Friction drag and heat transfer comparison between variable and constant fluid properties

The influence of variable fluid properties on friction drag $C_f(Gr_x)^{1/4}$ and heat transfer $Nu(Gr_x)^{-1/4}$taking along stream wise coordinate ξ is portrayed in Figure 2(a) and (b). This is done by comparing variable fluid properties with constant fluid properties when the $t^* = 0.0$ and $t^* = 0.01$. It is seen that skin friction slowly increases from zero and reaches its maximum value when $\xi = 3.0$ and then decreases with increases value of ξ . It is noticed that variable fluid properties increase friction drag and heat transfer as compared with constant fluid properties. Furthermore $C_f(Gr_x)^{1/4}$ for variable fluid property differs from constant fluid property by 8.1% when $t^* = 0.0$ at $\xi = 2.0$, but when $t^* = 0.01$ the same differs with 11.48% at $\xi = 2.0$. although in the case of $Nu(Gr_x)^{-1/4}$the variable properties differs from constant properties is 1.57% when $t^* = 0.0$ and 2.2% when $t^* = 0.01$ at $\xi = 2.0$. It is also remarked that variable fluid properties move zero skin friction downstream as compared with constant fluid properties.

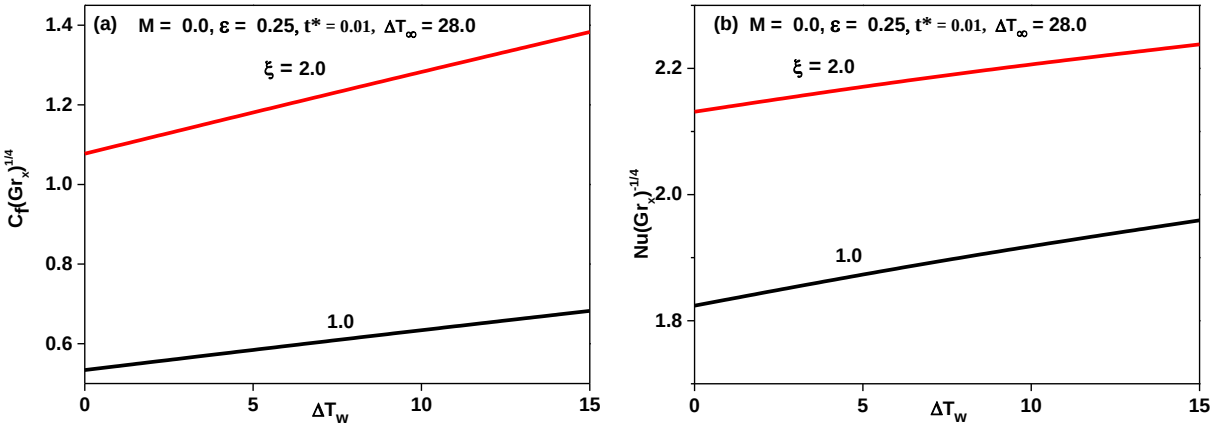

Figure 3. ΔT_w effects on (a) friction drag and (b) heat transfer parameters at different stream wise location

As we have considered that viscosity and Prandtl number are inverse function of temperature, the fluid and surface temperature difference is the main reason for variation of viscosity and Prandtl number inside the boundary layer. To notice this influence, friction drag coefficient $C_f(Gr_x)^{1/4}$and heat transfer coefficient $Nu(Gr_x)^{-1/4}$ are plotted against ΔT_w in the Figure 3.(a) and (b) respectively. The maximum value $\Delta T_w = 15^0C$ is taken to maintain the temperature within in the permissible value ($\leq 43^0C$), as $T_\infty = 28.0^0C$ with $\varepsilon = 0.25$. It is viewed from the Fig.3.(a)-(b), both friction drag and heat transfer rise with ΔT_w. It is also noted as ξ increases, both the coefficients increases.

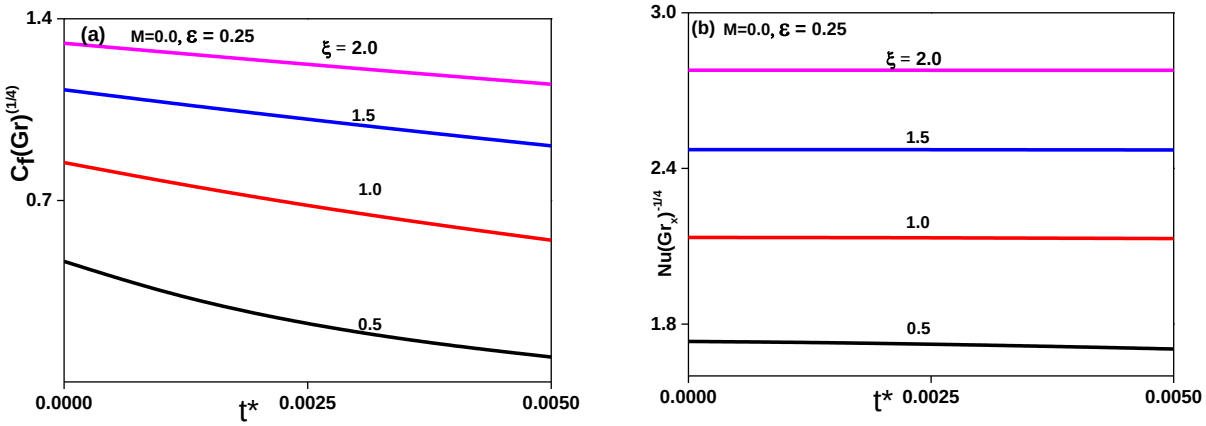

Figure 4. (a) Friction drag and (b) heat transfer parameters at various stream wise location

Figure 4.(a) and (b) depicts the effect of different stream-wise locations on friction drag $C_f(Gr_x)^{1/4}$and heat transfer $Nu(Gr_x)^{-1/4}$. It is perceived that as stream location(ξ) changes both friction drag and heat transfer increases. Moreover it is interesting to see that the monotonic decreasing trend of friction drag from different heights of the cylinder with the passage of time from $t^* = 0.0$ to $t^* = 0.01$ in the unsteady regime. This is due to dominance of variable viscosity and Prandtl number. But as time t^* progresses, heat transfer slowly decreases.

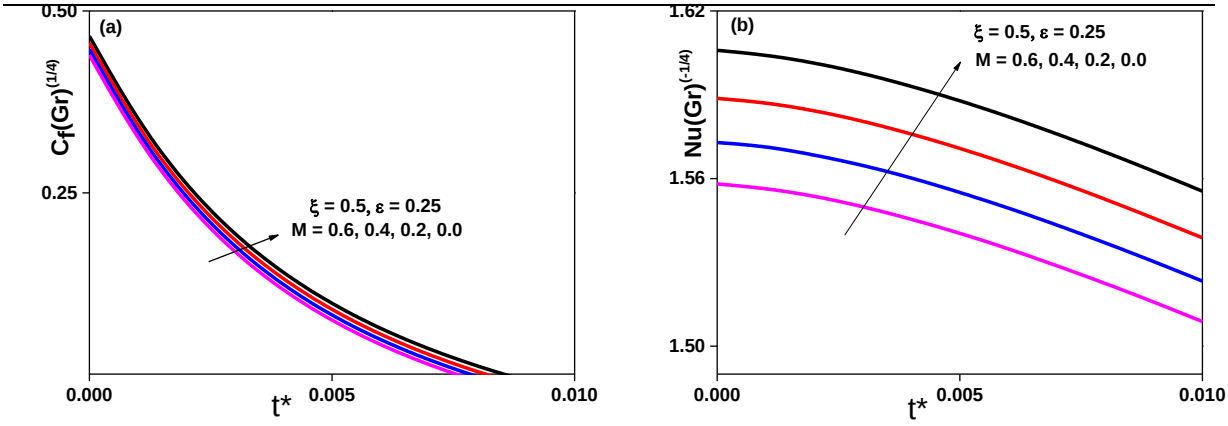

Figure 5. (a) Friction drag and (b) heat transform coefficient behaviour for different of magnetic parameter

To see the impact of the magnetic parameter on friction drag and heat transfer, Figure 5.(a) and (b) are plotted for $\xi = 0.5$, $\varepsilon = 0.25$ against time t^*. From the graph, it is perceived that friction drag and heat transfer as the magnetic parameter is enhanced. An enhancement of the magnetic parameter causes a force called the Lorentz force, which reduces the velocity and the temperature gradient of the fluid, hence friction drag and heat transfer decrease. However with the lapse of time friction drag diminishes significantly, decreasing rate tendency for the same is faster when $M = 0.6$ as compared with $M = 0.0$. The decreasing percentage of skin friction is 57.14% and 9.81% respectively when $M = 0.6$ and $M = 0.0$ at $t^* = 0.007$ and $t^* = 0.002$.

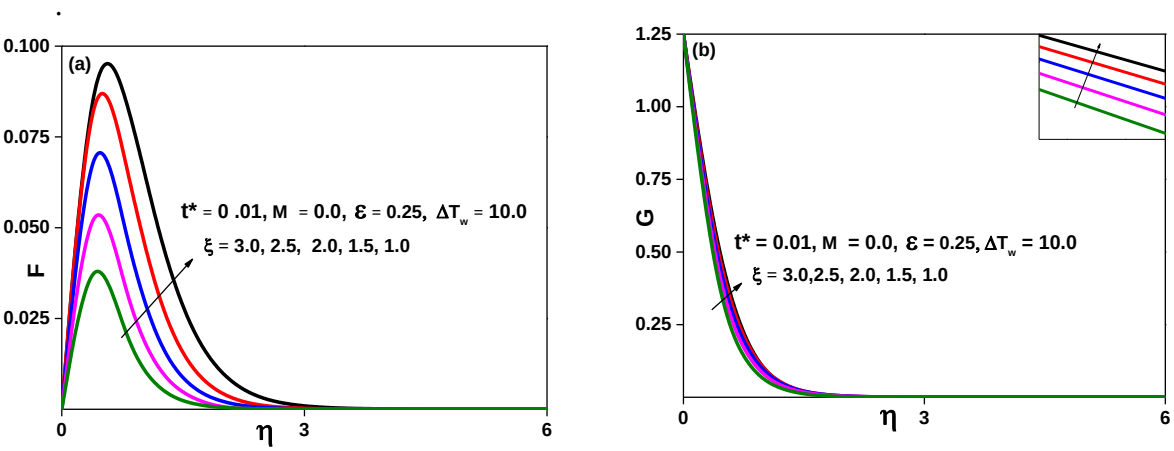

Figure 6. (a) Velocity and (b) Temperature profile at various stream wise location

The figure 6.(a) and (b) show the profile of velocity and temperature at various stream wise locations ξ at time $t^* = 0.01$, $\varepsilon = 0.25$ against η. It is seen from the Figure 6.(a) that velocity of the fluid gradually increases and reaches its maximum at $\eta = 0.4$. After that, it slowly decreases and then becomes zero. However, the flow is deaccelerated with increasing ξ. Figure 6(b) shows that thickness of the thermal boundary layer decreases as ξ increases, as a consequences of this, rate of heat transfer enhanced inside the boundary layer.

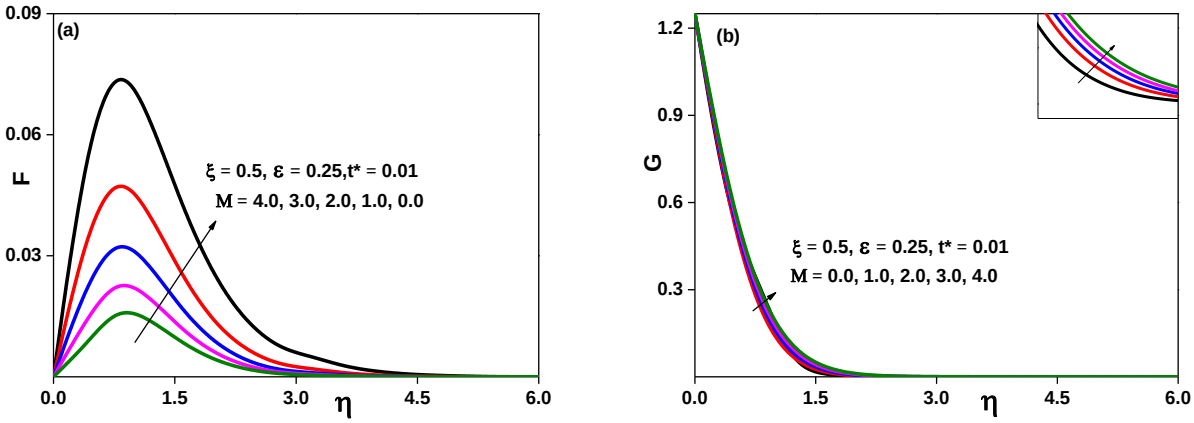

Figure.7. (a) velocity and (b) temperature profile for different values of magnetic parameter

Revelation of dimensionless velocity and temperature profile for magnetic parameter when $t^* = 0.01$, $\varepsilon = 0.25$ and $\xi = 0.5$ in contrary to η is taken in the Figure 7.(a) and (b). It has been observed that, rise in magnetic field declines the velocity of the flow, in fact as magnetic parameter is applied normally to the flow then there exits Lorentz force opposite to this field thereby retarding the flow velocity, consequently enhancement of thermal boundary layers takes places and thereby heat transfer rate declines in the boundary layer.

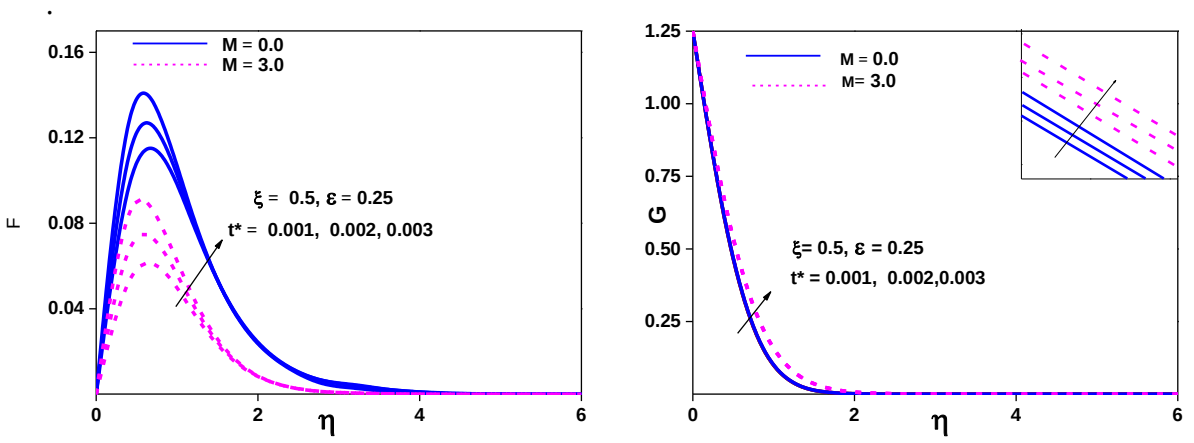

Figure. 8. (a) Velocity and (b) temperature profile for distinct values of t^*

The velocity and temperature behaviour of the fluid for different values of t^* and magnetic field is considered in Figures 8.(a) and 8.(b) respectively. It can be noticed that enhancement of t^* and magnetic parameter decreases the velocity profile, however the opposite of this is noted in the temperature profile. This true, as magnetic field is applied there exists a force which retards the fluid flow. As a result of this, there is declination in the thickness of both momentum and thermal boundary layer.

5. Conclusions

The unsteady MHD free convection of methanol flow over a thin cylinder with variable viscosity and Prandtl number has been analyzed numerically. The governing equations are resolved

by implicit difference scheme and quasilinearization technique. The graphical presentation of the computed values facilitates to bring out these following observations.

1. Variable fluid properties (viscosity) enhances friction drag and heat transfer and also moves zero skin friction downstream as compared with constant fluid properties.
2. The temperature difference between surface and fluid enhances both friction drag and heat transfer.
3. In different free stream locations, skin friction and heat transfer increase but velocity and temperature profiles decrease.
4. As magnetic parameter increases skin friction, heat transfer and velocity profile decreases, whereas opposite of this is seen in temperature profile.
5. Unsteadiness in the fluid decreases the velocity and increases the temperature profile.

Acknowledgement

The authors thank Principal and the Management of GSSSIETW, Mysuru for their support.

Nomenclature

x	axial coordinate
r	radial coordinate perpendicular to the axis of the cylinder
f	dimensionless stream function
F	dimensionless velocity
T, G	dimension and dimensionless temperature
g	acceleration due to gravity
r_0	radius of the cylinder.
u, v	velocity components in the x- and y-direction, respectively
t, t*	dimensional and dimensionless time
Gr	Grashof number
Gr_x	local Grashof number
Pr	Prandtl number
C_f	skin friction coefficient
Nu	Nusselt number

Greek symbols

ν	kinematic viscosity
μ	dynamic viscosity
ψ	dimensional stream function
η	similarity variable
α	thermal diffusivity
ρ	fluid density
ξ, η	transformed coordinates
ε	constant

Subscripts

w	condition at the surface (wall)
∞	free stream condition

Superscript

'	differentiation with respect to η

References

[1] C.D Surma Devi, M Nagaraj, G. Nat, Axial heat conduction effects in natural convection along a vertical cylinder. International Journal of Heat and Mass Transfer, 29, pp.654-656, 1986,
[2] H.S. Takhar, A.J., Chamkha, G. Nath, Natural convection on a vertical cylinder embedded in a thermally stratified high-porosity medium. International. Journal of Thermal Science, 41,83–93
[3] Md. A Hossain, R.K. Mondal, S.F. Ahmmed, A numerical study on unsteady natural convection flow with temperature dependent thermal conductivity past an isothermal vertical cylinder. International Journal of scientific research and management (IJSRM), 3, pp.3259-3265, 2015.
[4] H. P. Rani G. Janardhana Reddy, Chang Nyung Kim, The effect of the couple stress parameter and Prandtl number on the transient natural convection flow over a vertical cylinder. Acta Mechanica Sinica. 29, pp.649–656, 2013;
[5] P.Loganathan and B. Eswari, Natural convective flow over moving vertical cylinder with temperature oscillations in the presence of porous medium. Global Journal of Pure and Applied Mathematics, 13, pp.839-855,2017;
[6] Periyana Gounder Ganesan, Ponnamma Hari Rani, Unsteady free convection MHD flow past a vertical cylinder with heat and mass transfer.International Journal of Theral Science. 39, pp.265–272, 2000..
[7] Suresha Suraiah Palaiah, Hussain Basha, Gudala Janardhana Reddy, Magnetized couple stress fluid flow past a vertical cylinder under thermal radiation and viscous dissipation effects. Nonlinear Engineering, 10, 343–362, 2021.
[8] Hari Ponnamma Rani and Chang Nyung Kim, A numerical study on unsteady natural convection of air with variable viscosity over an isothermal vertical cylinder. Korean J. Chem. Eng., 27,pp. 759-765, 2010;
[9] C.Poornima, G. Ashwini and A.T. Eswara, Non-Uniform Slot Suction (Injection) into MHD Axisymmetric Boundary Layer Flow with Variable Viscosity. International Journal of Mathematics and Scientific Computing, 1,pp. 78-85, 2011.
[10] Oluwole Daniel Makinde., Effect of variable viscosity on thermal boundary layer over a permeable flat plate with radiation and a convective surface boundary condition. Journal of Mechanical Science and Technology, 26, 1615-1622, 2012.
[11] Rasool Alizadeh, Asghar B. Rahimi , Reza Arjmandzadeh , Mohammad Najafi , Ahmad Alizadeh, Unaxisymmetric stagnation-point flow and heat transfer of a viscous fluid with variable viscosity on a cylinder in constant heat flux. Alexandria Engineering Journal .55, pp.1273-1283, 2016.
[12] Ajibade AO and Bichi YA. Unsteady natural convection flow through a vertical channel: due to the combined effects of variable viscosity and thermal radiation. J Appl Computat Math.,7, 1000403, 2018.
[13] Amos S. Idowu , Mojeed T. Akolade , Jos U. Abubakar & Bidemi O. Falodun, MHD free convective heat and mass transfer flow of dissipative Casson fluid with variable viscosity and thermal conductivity effects. Journal of Taibah University for Science, 14, pp. 851–862, 2020.
[14] Ajay C K and Srinivasa A H, Viscous dissipation, radiation, heat source (sink), pressure work and mhd effects in boundary layers on continuous moving surface along with temperature dependent viscosity", Annals Of Mathematics and Computer Science, 3 pp. 30-50, 2021.
[15] A. Pantokratoras. Further results on the variable viscosity on flow and heat transfer to a continuous moving flat plate. International Journal of Engineering Science, 42, pp.1891–1896, 2000.
[16] Saikrishnan Ponnaiah," Boundary layer flow over a yawed cylinder with variable viscosity Role of non-uniform double slot suction (injection). International Journal of Numerical Methods for Heat & Fluid Flow, 22, pp. 342-356, 2012.
[17] Abhishek Kumar Singh, A.K. Singh and S. Roy, Analysis of mixed convection in water boundary layer flows over a moving vertical plate with variable viscosity and Prandtl number. International Journal of Numerical Methods for Heat & Fluid Flow, 29, pp. 602-616, 2019.
[18] K N Roopadevi, A.T. Eswara and A. H. Srinivasa, Variable viscosity and Prandtl number efect on mhd unsteady free convection axisymmetric ethanol boundary-layer flow, SN Computer Science, 4,382, 2023,
[19] Caracteristiques Physiques Des Fluides Thermiques Physical Data of Thermal Fluids.
[20] Property Tables and Charts (SI Units).
[21] Varga, R.S. Matrix iterative analysis, Prentice-Hall. 2000